STATUS REPORT ON THE TRANSMISSION LINE MAGNET

G.W. Foster,
Fermi National Accelerator Laboratory, PO Box 500 Batavia IL 60510
September 29, 1997

Abstract

The current status of the design of the "Double-C" transmission line magnet is reviewed. Technical notes describing prototype results, design changes, and performance calculations are cited. Open design issues, the ongoing R&D efforts, and plans for the next round of prototypes are discussed.

1 INTRODUCTION

A cross section of the Transmission Line Magnet [1] design is shown in figure 1. It is a 2-in-1 warm-iron superferric magnet is built around a 75kA superconducting transmission line. The current is returned in the cryogenic distribution lines located in a structural tube underneath the magnet. Steel yokes above and below the transmission line concentrate the magnetic flux in a pair of gaps which provide opposite bend fields in the twin apertures needed for P-P collisions. The pole tips are shaped to provide the alternating gradient necessary to focus the beams, thereby eliminating quadrupoles and allowing the magnet to be continuous in long lengths. All vacuum hardware, instrumentation, and cryogenics are pre-assembled and tested in the factory. The length of the magnet assembly is ~250m (four half-cells).

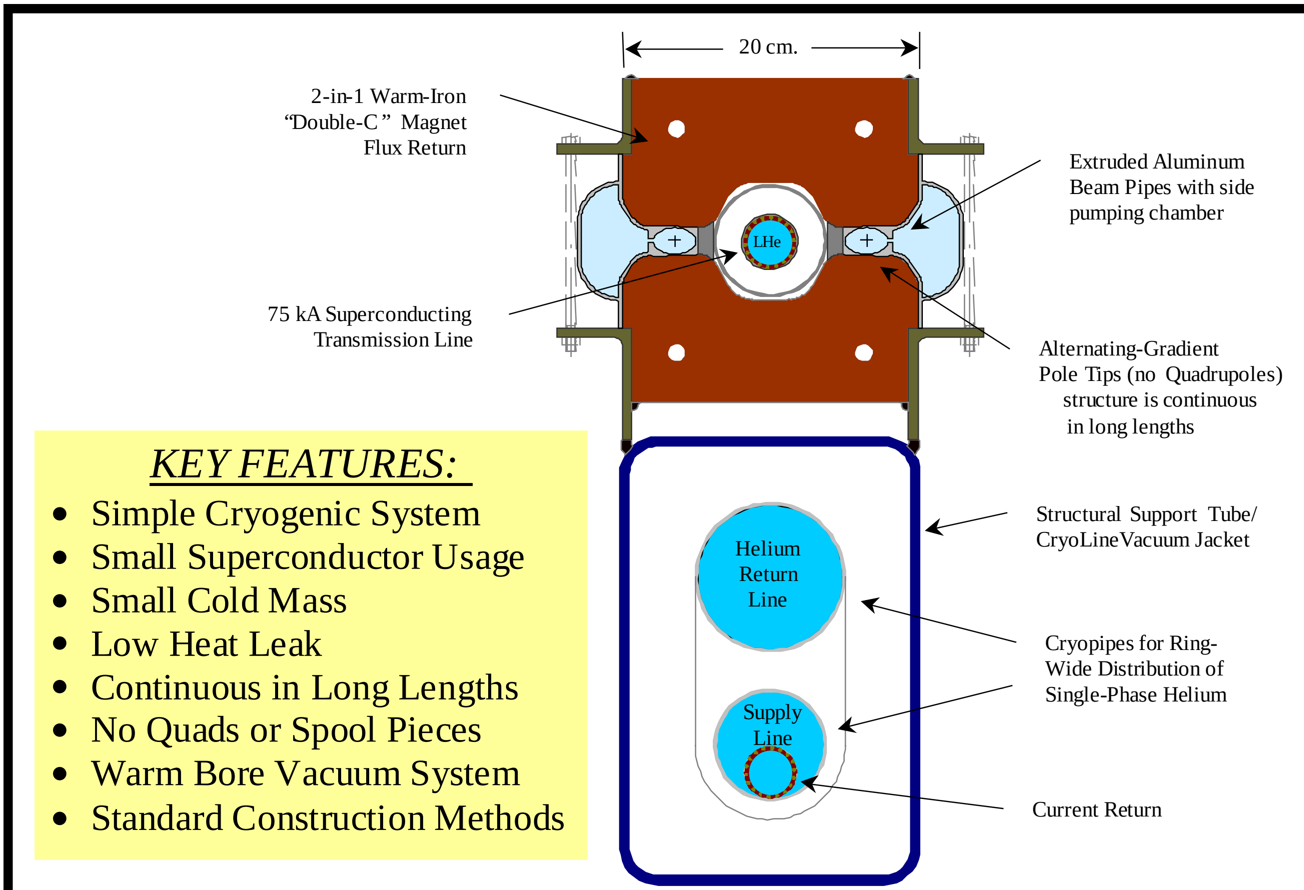

Figure 1 - Transmission Line Magnet

This design is believed to address all mechanical, cryogenic, electrical and beam dynamics constraints for both the 50x50 TeV VLHC and the 3 TeV injector. A 2m long model magnet built to test various aspects of the assembly procedures is shown in Fig. 2. We are currently ordering parts for the next (~50m long) prototype based on this design.

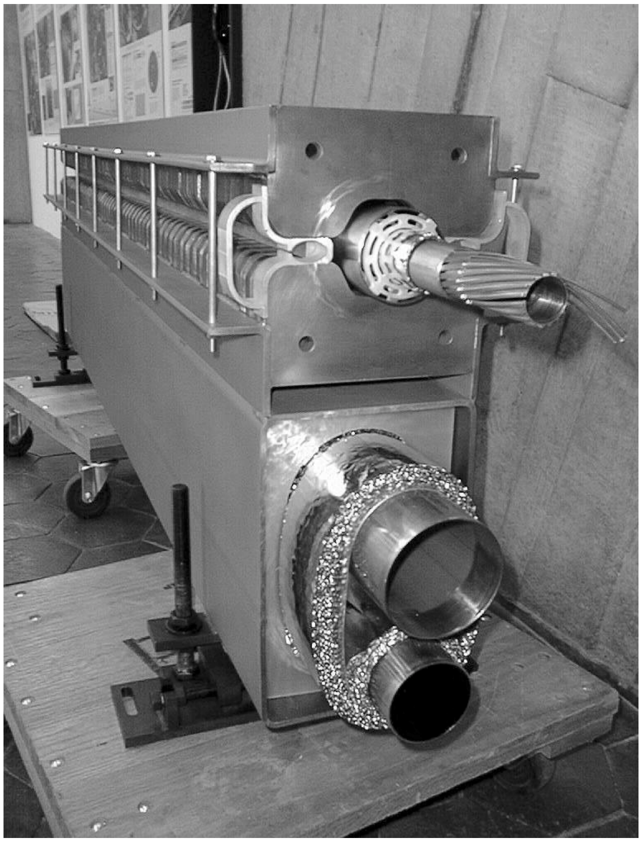

Fig. 2 - Photo of 2m Model. This design will be used for the 50m prototype.

A table of parameters for the transmission line magnet is given in Table 1.

Magnet Type	Warm Iron, Warm Bore
Magnet Topology	Double-C, 2-in-1
Operating Range	0.1T → 2T
Drive Conductor	Single turn, 75 kA Superconducting Transmission line
Focusing	Alternating-Gradient Combined Function (no quads or spool pieces)
Normalized Gradient	5%/cm for a typical lattice
Magnet Aperture	3cm x 2cm (H x V)
Good-Field Aperture ($\lvert\delta By/Bo\rvert < 10^{-4}$)	2cm round at injection 1cm round at 2T
Iron Dimensions	20cm x 20cm
Transmission Line	7.5cm diam x 250m length
Inductance	2.3uH/m (low currents) 1.9uH/m ($2E_S/I^2$ at 75kA)
Iron Yoke	Laminated Low-carbon Steel

Table 1. – Transmission Line Magnet Parameters

2 FIRST PROTOTYPE SYSTEM

A short prototype system (Fig. 3) was built and operated under the guidance of Peter Mazur, stewardship of Cosmore Sylvester, and with instrumentation built by Phil Schlabach. A paper [2] on results from the first test run of the prototype system was presented at the 1997 PAC (Particle Accelerator Conference) and is included in these design notes. The system included a 5m loop of superconducting transmission line, a current transformer, and a double-C magnet iron yoke 1m long. The current transformer was used to excite a large circulating current in the superconducting loop. This approach was used because it avoids the expense of large superconducting current leads. The system worked as expected, with the magnetic and electrical behavior of the current transformer, flux reversing switch, and double-C magnet behaving as calculated [3].

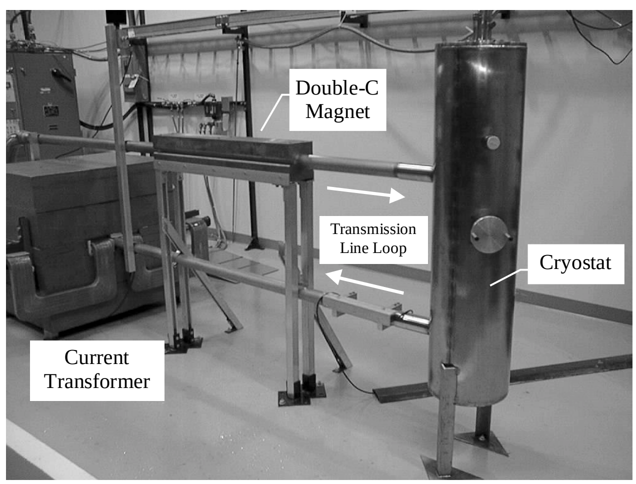

Fig. 3 – Photograph of the first prototype transmission line magnet.

The superconducting transmission line conductor quenched at a somewhat lower current than expected (43kA vs. 50kA design). The cause of this is believed to be that the conductor bundle (7 loops of leftover SSC cable) was essentially unconstrained in sections of the transmission line cryopipe. In subsequent designs the conductor will be continuously soldered to a monolithic copper stabilizer and this should be avoided.

3 MAGNETIC DESIGN

The magnetic design of the double-C magnet is essentially unchanged from the Snowmass [4] design. See Fig. 4. Field lines circulating around the transmission line are concentrated into the beam gaps by the iron pole tips. Saturation of the steel limits the field in the gaps to 2T at 75kA drive current and 2.2T at 100kA.

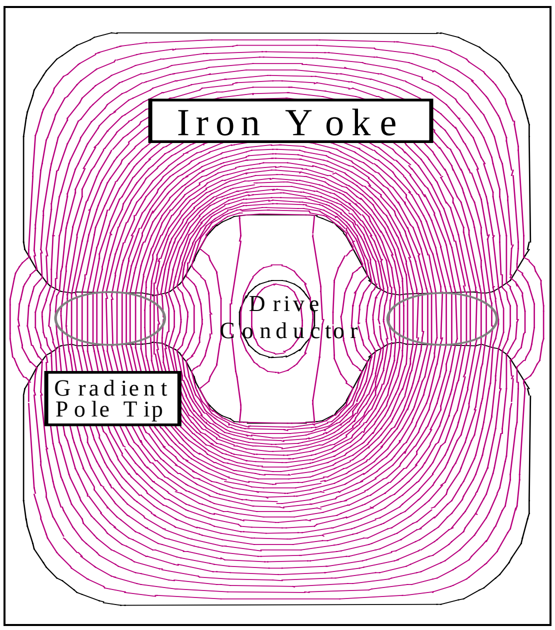

Fig. 4 – Magnetic field map of the transmission line magnet generated by POISSON. The small field gradient (~5%/cm) is visible in the pole tip shape.

The design features a "crenellated" pole tip [5] to mitigate saturation effects up to ~2 Tesla. This technique (Fig. 5) reduces the average density of the iron in the low-field regions of the pole tip, so that the pole saturates evenly. This preserves the field quality at much higher excitations (perhaps as high as 2.2T, see Fig. 6) than would be possible in an all-iron magnet.

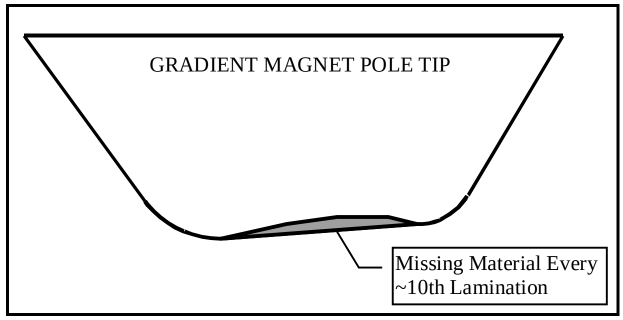

Fig. 5 - The "Transverse Crenelation" technique to minimize field shape changes from saturation.

The 2m laminated iron model in Fig. 2 has been constructed with one of its bores crenellated and the other without. This will be used for magnetic testing to verify the crenellation concept.

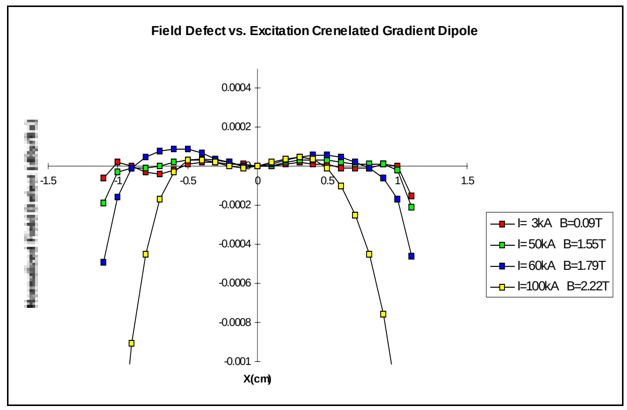

Fig. 6 - POISSON calculation of normalized field defect vs. horizontal position at different excitation currents for the crenelated pole tip design. The uncorrected field defect is below $\pm 10^{-4}$ across the ± 1 cm aperture for fields up to 1.8T. The goal of the R&D program is to demonstrate a design with acceptable field quality above 2T.

A "Double-C" iron test stand[6] with a drive conductor using water-cooled copper coils is being built by A. Makarov of the FNAL Technical Division to allow rapid turnaround of magnetic measurements. See Fig. 7. This will allow optimization of the pole tip shape, crenellation patterns, as well as the study of various correction strategies.

The magnetic measurement systems to be used on the transmission line magnets will also be developed on this test stand. The leading candidate is a stretched-wire system using support arms that reach into the gap of the C-Magnet. A rotating coil becomes difficult due to the scaling of pickup coil tolerances vs. coil aperture. Arrays of Hall probes are also being considered. A key issue is the presence or absence of the beam pipe as the long magnet assemblies are measured.

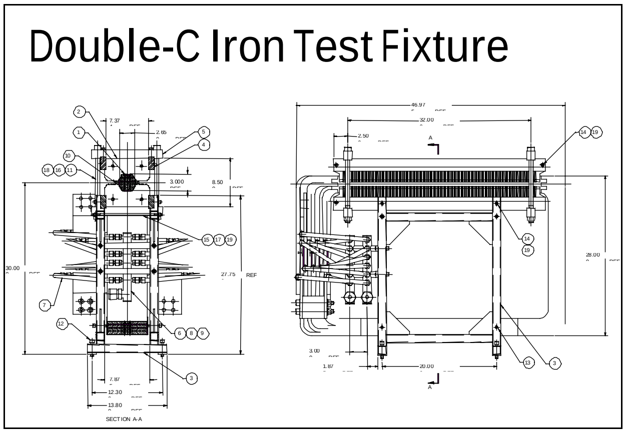

Fig. 7 – Design of the water-cooled copper test stand for optimizing the Double-C iron shape and developing appropriate measurement techniques. The fixture is electrically interchangeable with the Main Injector Dipole test stand at Fermilab's Magnet Test Facility. The coil is capable of putting 100kA-turns through a 3" diameter hole and driving the Double-C iron yoke far into saturation.

Another significant ongoing effort is to quantify the effects of variations in steel properties on the performance of the magnet. B-H data using the full production run of magnet iron for the Fermilab Main Injector is being used. Production trimming techniques to compensate for variations in strength and saturation properties of the magnet iron are being investigated numerically in POISSON.

Another area of work involves the alignment tolerances and decentering forces of the transmission line drive conductor. The present design requires alignment of the drive conductor within ~0.5mm of the magnet center[7]. This is felt to be doable, but we may change our mind after building and measuring the conductor centering in the first long prototype.

Preliminary magnetic designs exist for the 2-in-1 Lambertson [8] for beam extraction and abort. These magnets will be powered from the transmission line current so that they track the arc magnets and the beam energy. No separate power supplies or LCW connections are needed. Similar designs for the beam separation dipoles and straight-section quads will be developed.

The presence of the nearby iron in the structural support tube does not cause difficulties. This iron saturates completely at a very low excitation currents (well below injection energy) and does not contribute significantly to the stored energy or inductance at high field. The main detrimental effect of the iron support tube is to create an anomalous high inductance at low excitation currents. This makes it difficult to measure the electrical parameters of prototype magnets, and increases the size of the current transformer needed to drive long prototype magnets.

Two minor design changes are contemplated. Firstly, the gradient of the magnet will be reduced from ~5%/cm to 3%/cm to correspond to the lattice design for the 3 TeV injector[9]. This simplifies the design slightly. The second possible change is to increase the inner diameter of the iron by 1-2cm to allow additional insulation space for the transmission line vacuum jacket. This increases the iron cost somewhat but may prove cost-effective when cryogenics costs are factored in. It also reduces the conductor forces and loosens assembly tolerances on the centering of the conductor.

4 MAGNET APERTURE

Various concerns have been expressed regarding the sufficiency of the (2cm x 3cm) magnet gap of the proposed design. These include concerns over beam instabilities at injection energy, closed orbit distortions, magnet alignment and tunnel settling, the need for additional working aperture for beam injection and extraction, the need for additional horizontal aperture to perform resonant extraction for fixed-target operations, and the possibility of Pbar-P collisions in a single aperture.

Each of these items has been addressed, and the magnet aperture of the existing design is sufficient. (Pbar-P will require a separate set of magnets due, among other things, to limitations from the long range beam-beam tune shift). A companion note[10] discusses aperture requirements in more detail.

The two beam instability issues have been resolved as follows. The damper system to control the resistive wall (RW) coupled-bunch instability has been described by Marriner[11]. The damper system relies on proven technology, is not expensive, and does not require a 1-turn delay or across-the-ring signal transmission. Such a system has already been successfully demonstrated in the Fermilab Main Ring. The second (TCMI) instability is more conjectural since it has never actually been seen in a hadron machine. Like the RW instability, it is only a potential problem at injection energy into the large ring, and only for the high-luminosity ($L > 10^{34}$) scenarios. If it does become a problem, a straightforward workaround (due to Malamud[12]) is to inject and accelerate the charge in a number of high frequency RF buckets, then coalesce the beams into their final intense bunches at full energy. This reduces the bunch current at injection to a level below the TMCI thresholds. This type of coalescing is routinely done in FNAL collider operations and is an essential ingredient in achieving high luminosities in the Tevatron. Therefore, beam instabilities are not a problem for the 2cm aperture.

Magnetic field quality (dynamic aperture) at injection should not be a difficulty assuming that the normal field quality obtained in iron-dominated magnets is achieved. A properly designed iron magnet operating at 1 kG (the VLHC injection field) will typically have a dynamic aperture larger that the physical aperture of the magnet [13]. In other words the good-field region of iron magnets goes all the way up to the pole tip. This is in contrast to standard (conductor dominated cosΘ) superconducting magnets, in which the coil must be located a couple of cm outside of the good field region to maintain adequate field quality. Thus the good-field area (roughly defined by the area in which the total field defect exceeds 10^{-4} of the bend field) of the Transmission Line Magnet significantly exceeds that of (for example) the LHC dipoles at injection energy.

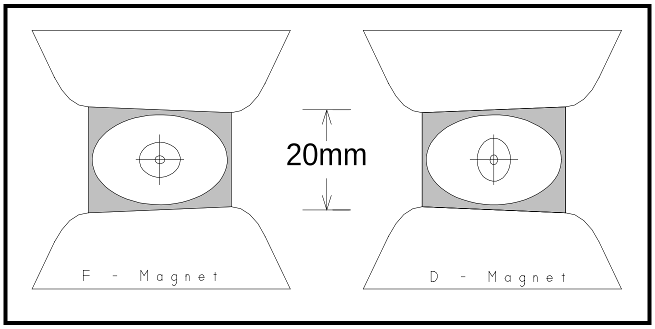

Fig. 8 - Beam Sizes in the 3 TeV Injector. The 95% beam envelopes for 15π beams (roughly the current FNAL collider emittances) are shown. The large ellipses show the beam envelope at injection energy (150 GeV). The small ellipses show the beam size at flattop (3000 GeV). The left and right pictures indicate the beam envelopes in the in the vicinity of focussing and defocusing half-cell locations. Lattice functions are β min =130m, β max = 200m, Dx = 6m. Beam sizes - 150 GeV: Rmin=3.5mm, Rmax=4.3mm; 3000 GeV: Rmin=0.8mm, Rmax=1.0mm. The magnet gap is 20mm x 30mm (h x v) and the beam pipe aperture is 18mm x 27mm. Beam sizes in the 50 TeV machine are roughly 2x smaller.

The physical aperture of the beam pipe is also a concern. The current beam pipe has an excess radial aperture of ~5mm (see Fig. 8 and Table 2). Here the excess radial aperture is the nominal aperture outside of the 95% beam envelope, for beams at injection energy, with the current emittances used in the Fermilab collider (15π in FNAL units). The situation improves when the beam is accelerated. It improves when one gets away from the β-max values encountered at each BPM. It improves if one considers the 50x50TeV machine where the beam sizes are ~2x smaller. It will improve further if (as expected) the emittance of the FNAL injector continues to decrease. The issue is then what aperture losses are anticipated from closed orbit distortions, magnet misalignments, etc.

	Horizontal	Vertical
15π 95% beam size @β-max, dP/P=.01%	± 4.4mm	± 4.3mm
Closed orbit distortion	± 0.5mm	± 0.5mm
Injection Steering Errs	± 1mm	± 1mm
BPM Offsets	± 0.1mm	± 0.1mm
Magnet Straightness	± 0.5mm	± 0.5mm
Magnet Settling (between realignments)	±1.0mm	±0.5mm
TOTAL	± 7.5mm	± 6.9mm
Available Aperture	± 10mm	± 9mm

Table 2 – Aperture at injection into the 3 TeV machine.

The 3 TeV machine does not need extra aperture for allowing kicked beams to propagate off-center through the arcs. (Several machines at FNAL do this). This is because it has zero-dispersion straight sections with enough length to contain both the kicker and Lambertson. It does not need helical orbits for Pbar-P since this would be done using two sets of magnets. Thus only on-axis orbits need to be considered in the arc magnets.

Closed orbit distortions are largely an issue of corrector strength, beam position monitors, and software. We assume that adequate corrector strength will be available to control orbit errors at injection. In the Tevatron, closed orbit distortions are generally kept under 1-2mm, which is adequate given the physical aperture of the machine. At LEP (where beam centering in the quads is more important due to radiation damping) they do ~0.1mm [17]. DESY does 0.05mm [14]. We assume in table 2 that a closed orbit distortion of 0.5mm will be achieved.

The aperture allowance for injection steering errors has been considered. Here the issue is the short-term reproducibility of the beam transfer kicks, since the injection orbit can be verified immediately before filling via low intensity pilot shots. The reproducibility of the injection orbit is currently <0.1mm for the Tevatron [15]. (It is worth noting that the warm-iron magnet should not be as sensitive to quenching from a mis-steered pilot shots as the Tevatron or other cold-bore machines.) Thus the allowance of 1mm in table 2 seems reasonable.

Beam Position Monitor (BPM) offsets will contribute to the aperture budget. Gross errors in BPM centering can be verified *in situ* with aperture scans which scrape either side of the aperture in the vicinity of each BPM. Again, the warm-iron magnet should tolerate aperture scans better than cold-bore superconducting magnets. The 0.1mm allowance in table 2 corresponds to ½% position accuracy in the BPM readout.

Kinks in the magnet bore will reduce the available aperture. The assembly tolerances are discussed in ref 16. The straightness tolerance (R&D goal for the 50m prototype) is ±0.5mm. Survey of the magnet bore is straightforward since the position of the aperture can be surveyed to ±0.25mm at any place along the length of the magnet via fiducial notches on the warm iron laminations. Alignment feet allow the magnet bore to be re-centered on the beam every 6m along its length. Between the supports, the magnet assembly must be straight to the required tolerances. It should also be noted that the straightness tolerance only applies to the bore in the vicinity of the focussing BPM in each coordinate, and is relaxed at other points nearer the beam waist.

Tunnel settling will be another source of kinks in the magnets that develop over time. Tunnel deformations with a distance scale longer than the BPM/corrector spacing can be compensated for by reprogramming the correctors or moving magnets. Tunnel deformations between the BPM's will reduce aperture and must be corrected for by periodically realigning the magnets. Current thinking is to have a semi-automated mechanism which regularly surveys and realigns the magnets them so that they are straight between the BPM's. The tunnel settling straightness tolerances in Table 2 reflect estimates based on the random movement of quadrupoles in the SPS tunnel [17] over a 2-year period between alignments. See Ref. 16.

Resonant extraction aperture requirements for fixed-target operations from the 3 TeV injector have been calculated by Marriner[18]. This does not affect aperture requirements at injection since extraction takes place at flat top; however it often gets mentioned as a possible reason to need a bigger beam pipe. Optimized resonant extraction involves spreading out the beam in whatever horizontal aperture is available. Only the horizontal physical aperture is relevant rather than the good-field aperture since the high-amplitude resonant particles in the beam are lost after only a few turns. Vertical aperture requirements are not increased. The beam is extracted at a localized high-beta insert in a straight section in order to make the septum width (measured in beam sigmas) as small as possible. Assuming a 1:4 ratio between the β-functions in the arcs and the extraction septum, Marriner calculates that acceptable extraction efficiencies of 99% can be obtained. If necessary, this extraction efficiency could be increased further by increasing β at the extraction septum. Thus the current beam pipe dimensions are sufficient for high-efficiency resonant extraction should this be desired.

Another possible concern is that the lower energy beams of the 3 TeV injector may require a somewhat larger aperture than the 50 TeV VLHC itself. This would prohibit a common magnet design for both machines. For lattices under consideration[19], the betatron beam sizes in the injector are roughly 2x smaller in the 50 TeV VLHC. However the injector benefits from a number of mitigating factors, including the feasibility of stronger beam orbit correctors, a more favorable situation with respect to beam instabilities, a smaller dwell time at injection, and the relative ease of survey and alignment. Thus the present design appears suitable for both.

5 MECHANICAL DESIGN

A significant design change since Snowmass is the switch from extruded steel to laminated iron half-cores. This is an important decision since ~2/3 of the magnet cost is in the iron yokes. This change was driven by several factors. Firstly, the 3 TeV injector may have a ramping time as short as 10 seconds, and the eddy-current-induced field defect from a solid iron pole tip would require strong correctors[20]. A second factor was that implementing the crenellations in the pole tip is much easier in a laminated magnet than in an extruded magnet, and does not require special tooling. A third consideration is that we were able to obtain very attractive pricing for assembled, stacked, and crenellated half-cores from the same vendors who produced the Main Injector magnets.

For the 50 TeV machine we expect that the extruded/cold drawn steel yokes will be significantly less expensive. Eddy currents are not a problem for the 1000 second ramp time of the 50 TeV machine. Extruded steel pole tips were used successfully for quadrupole production for Fermilab's Recycler Ring, and gradient magnet pole tips have been produced for the Recycler which meet the required ±0.0002" tolerances on the pole tip shape. The learning curve on the extrusion/cold draw process was steep. We feel however that it is expedient to adopt a conventional baseline design using traditional stacked and welded laminations for the cost estimate as well as the next round of prototypes.

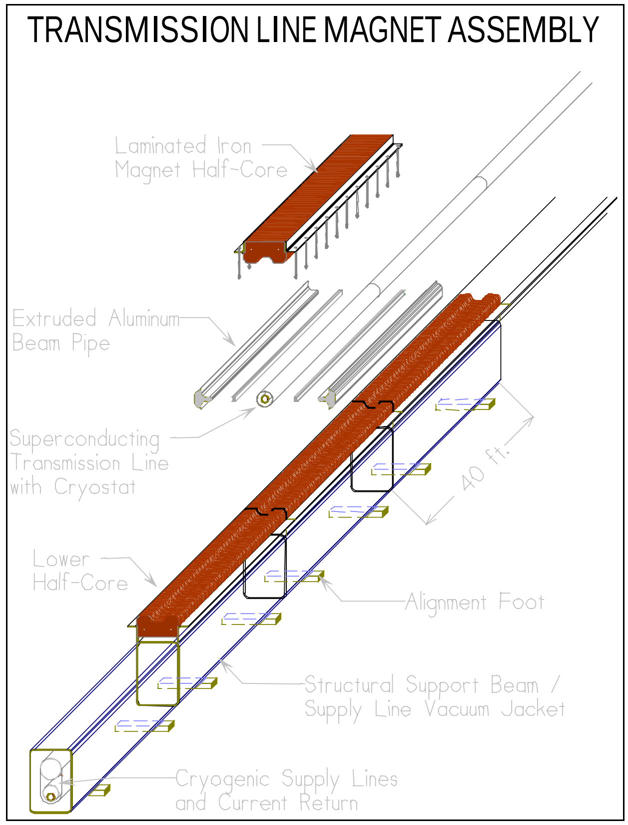

Fig. 9 – Transmission Line Magnet Assembly.

A structural support beam [see Fig. 9] is required to support the laminated iron structure. This support beam also serves as the vacuum jacket of the cryogenic distribution lines. The combined structure is rigid enough that supports every 6m (20') are sufficient to align the structure. Support and alignment tolerances in the Transmission Line Magnet assembly are discussed in Ref. 21.

Thermal expansion forces on the support beam are a significant engineering issue. The current plan is to mechanically connect the support beams between magnets. It thus becomes a continuous mechanical element analogous to continuously welded railroad rails (which go 100's of km between cities without thermal relief). However these longitudinal forces must be periodically anchored to the rock (e.g. at the ends of the magnets) to prevent fault conditions from damaging long lengths of magnets. Maintaining transverse alignment tolerances in the presence of these longitudinal forces will require engineering attention and prototype work.

The mechanical stability of the transmission line cryopipe is another significant engineering issue. The challenge is to support the cryopipe with the lowest possible heat leak in the presence of decentering magnetic forces. (Although there are no magnetic forces on the drive conductor when it is at its nominal center position, there is a decentering "negative spring constant" which means that the drive conductor will be attracted to the top or bottom of the iron yoke when it becomes vertically off center). The situation is analyzed in Ref 28.

6 MAGNET ASSEMBLY

A baseline magnet assembly plan has been defined which makes maximum use of products from commercial vendors while maintaining final assembly and Q/A under control of Fermilab. The goal is to minimize on-site infrastructure and tooling costs. The situation should be similar to the case of Main Injector magnets, in which 95% of the value added came from outside vendors and only 5% of the costs were from on-site assembly and Q/A.

Major components are pieced together from commercially produced 40-foot lengths: the pre-assembled laminated half-cores, the structural support tube, the Invar transmission line cryopipe, vacuum jacket, and the cryogenic transfer lines. The choice of 40-foot lengths allows truck shipment to the final assembly site.

This approach is similar to the construction of the ~8km of cryogenic transfer lines for the Fermilab Tevatron. The construction of the cryo transfer lines (which were pieced together from long lengths at an on-site factory) was completed quickly and at a cost that was dominated by the parts cost. They have operated for 13 years without failure.

The superconductor and copper stabilizer must be continuous for the full length of the magnet. This is accomplished by commercially fabricating the copper stabilizer and superconducting strand into strips 10cm x 3mm x 250m long. The strip is transported on 750ft, 1500-lb. reels to FNAL where a final roll-forming operation converts the strip into a helical coil.

7 TRANSMISSION LINE DESIGN

Considerable progress has been made at arriving at a baseline design (

Fig. 10) which satisfies all known requirements while relying as much as possible on normal commercial processes.

Design constraints include carrying the 75kA current with adequate margin, handling thermal contraction, quench protection, hydraulic impedance, manufacturability, splicing, heat leak, conductor centering, and control of conductor forces. A cross section of the transmission line conductor is shown in Fig. 12.

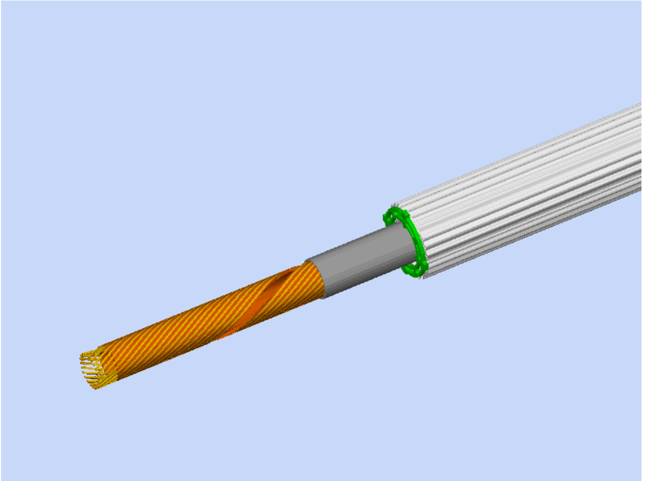

Fig. 10 – CAD rendering of the superconducting transmission line. From left to right: superconducting NbTi strand, helically slit copper stabilizer, invar cryopipe, G-10 cold-mass support "spider", and aluminized-mylar superinsulation. Not shown: stainless steel vacuum jacket and vacuum breaks

The superconductor consists of 18 strands of 2mm diameter copper-stabilized NbTi with a Cu:SC ratio of 1.3:1. The conductor operates in essentially a self-field of 0.8 Tesla, even when there is 2T on the pole tips (see Fig. 4). Fine filaments are not required since persistent current effects are unimportant in an iron-dominated magnet. The operating current is 75kA at an operating temperature of 7K. Enough superconductor is included to operate at 100kA if the cryogenic system operates with 6°K peak temperature in the drive conductor.

Figure 11 – Photograph of transmission line conductor at end of 2m model magnet. From left to right: NbTi superconducting strand, helically-slit copper stabilizer, Invar cryogenic pipe, vacuum superinsulation, G-10 support "spider", 304 Stainless Steel vacuum jacket, and body of transmission line magnet.

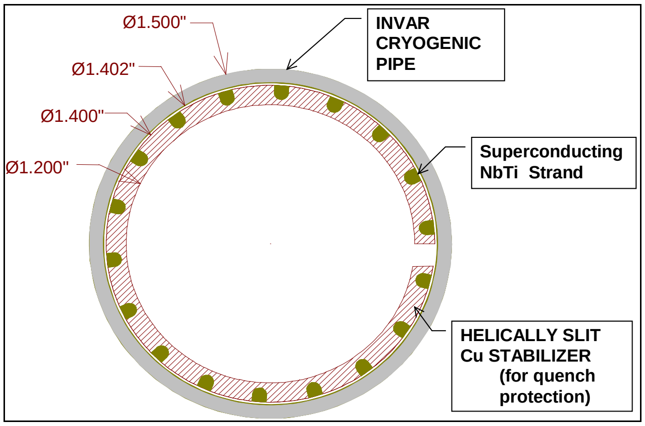

Fig. 12 - Transmission Line Drive Conductor

Operating Current	75kA
Operating Temperature	4.5-6.5K
Operating Field	0.8 Tesla
Superconductor	2mm NbTi Strands
Number of Strands	18 strands at 20°Spacing
Strand Diameter	2 mm
Copper: SC ratio	1.3:1
Cryopipe	1.5" Drawn Tube
Material	36% Nickel Steel (Invar)
OD/ID/Wall	1.5" / 1.402" / 0.049"
Manufacture	Assembled (orbital welded) at FNAL from 40ft lengths
Copper Stabilizer	Helical Slit copper tube
OD / ID / Wall	1.400" / 1.200" / 0.100"
Alloy	OFHC
RRR	55 (min, after cold work)
Helix Pitch	3-5 turns/meter
Strand Attachment	Soldered to stabilizer

Table 3 – Transmission Line Conductor Parameters

8 INVAR CRYOPIPE

The Invar cryopipe of the transmission line drive conductor solves several problems in the design of the drive conductor. The main benefit of Invar[22] is that its low thermal contraction to cryogenic temperatures (approximately 1/7 of 304 stainless steel) eliminates the need for cryogenic bellows. This permits a compact design and a lower heat leak. It also minimizes or eliminates abrasion problems on the drive conductor and support spiders.

In its planned use, the Invar cryopipe will be physically constrained at the vacuum breaks at the ends of the transmission line segments. Under these circumstances cold Invar goes into modest tension (7 kPSI stress) which is well below its yield point (120 kPSI at cryogenic temperatures). In the Invar can then be thermally cycled repeatedly to cryogenic temperatures without damage.

There are however several potential concerns in our application of Invar. Firstly, Invar is reputed to be difficult to weld, although problems occur mainly in connections to dissimilar steels. We must ensure that our welding procedures produce welds that survive repeated thermal cycling, under tension, without loss of reliability. Secondly, adequate dimensional stability of the Invar should be verified after repeated thermal cycles. There is mention in the literature that Invar changes length slightly for some period following cold work. Finally, Invar it is not a true stainless steel and it can rust.

For these reasons, as well as to gain experience in handling Invar before committing to a prototype, we are arranging the simple test setup in Fig. 13. A 50m length of Invar piping with a large number of girth welds will be clamped on either end, then thermally cycled by flushing alternately with liquid nitrogen and room temperature nitrogen. Warm strain gauges will monitor the forces from thermal contraction. The leak-tightness and length of the pipe will be checked before and after hundreds of thermal cycles.

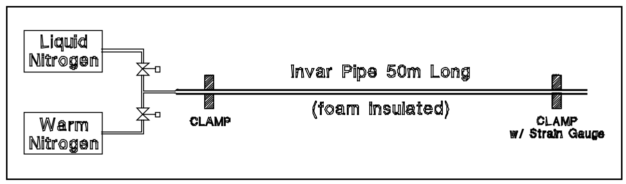

Fig. 13 – Invar Cryopipe test setup.

Invar is ferromagnetic (B_{SAT} ~0.8T) and will fully saturate at low currents in the drive conductor (below injection energy). It is not believed that this will cause any difficulties.

9 HELICAL COPPER STABILIZER

The superconductor/copper stabilizer structure has a helical slit (see

Fig. 10). This serves three purposes. Firstly, it avoids mechanical damage during cryogenic cool down. The slit provides a "springiness" which, if not present, would cause excessive stress and yielding in the copper. This cold work would mechanically and electrically degrade the copper and superconductor. Secondly, the helical structure allows the copper/superconductor structure to be shipped in strip form on reels to FNAL, then formed into the helically slit pipe in a single roll forming operation. This minimizes the on-site labor content of the transmission line and allows the use of commercial processing for the copper fabrication, plating, and soldering of the superconducting strand. Thirdly, the helical slit provides a structure that can be shrunken radially by twisting it up (like a rubber band). This permits an assembly procedure in which a long section of copper helix is twisted up to reduce its radius. Forty-foot sections of Invar pipe are then slid over the copper structure and welded into a continuous length, and finally the torsion on the copper is released so that it fits snugly into each section of Invar pipe. This assembly procedure is being tested on dummy copper helix and stainless pipe sections.

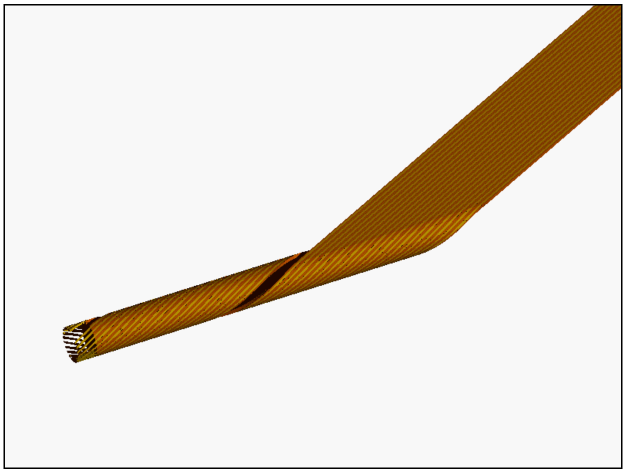

Figure 14 – Roll forming operation which converts the copper strip containing the superconducting strand into a helically-slit pipe. The strip arrives on reels from a commercial vendor and is roll-formed on site. The helical twist is necessary so that the pipe can sustain cool down to cryogenic temperatures without damage.

A finite element analysis [23] of the thermal stresses of the copper helical structure was made. The total force necessary to constrain the copper to a fixed length on cool down was calculated. This force was found to vary roughly as 11000kgf/N^3, where N is the number of helix twists per meter. Choosing N=4 twists per meter gives a tension of 690kgf. This is less than the thermal tension on the Invar pipe (~750 kgf).

To verify the calculations, a mechanical sample of the helical copper structure was prepared and tested in the Instron machine at the FNAL Materials Testing Laboratory. The sample was 1m long with a helix pitch of 2 turns/meter. The elastic modulus agreed within 20% with the finite-element analysis.

There are several unresolved issues in the transmission line conductor design. The electrical insulator that isolates the transmission line from the rest of the magnet can be warm or cold, inside or outside the cryopipe and/or vacuum shell. The copper stabilizer may be a monolithic helical pipe or a series of interlocking but mechanically independent pieces. The helix pitch of the conductor is not yet set and will depend on further calculations and experience with the long prototypes. These issues are more in the nature of cost optimizations rather than fundamental questions about the feasibility of the design.

10 AUTOMATIC WELDING

We have tested Fermilab's automatic orbital welders for use in assembly of the cryogenic piping. The performance is excellent on both Invar and stainless steel. The weld on the transmission line cryopipe can apparently take place directly over the copper/superconductor structure without damaging it. This success is significant because it opens up a number of convenient options for manufacturing and splicing the transmission line conductor.

Fermilab also owns larger orbital welders for sectioning together the structural support beam and cryostats. These will be used building the 50m prototype.

11 TRANSMISSION LINE SPLICE

The ability to make simple and reliable *in situ* splices in the transmission line is essential. The procedure is as follows. First, the magnets are moved into position and the two ends of the transmission line conductor are brought together. It is not necessary that transmission line ends line up exactly, and a gap of 1-2" between the copper pipe stabilizers is allowable. The ends of the copper structure are modified so that each corresponding pair of strands of superconductor can lay alongside each other in a common channel in the copper. The strands are laid alongside each other and soldered using a clamping fixture analogous to the soldering fixture developed for Tevatron cables. Next, a pair of copper half-pipe sections are clam-shelled and soldered around the joint. This provides the electrical continuity of the copper stabilizer necessary for quench protection of the splice. A telescoping section of Invar cryopipe is then orbitally welded over the splice. This joint is leak checked using methods developed by Mazur [24] for externally leak checking a pipe-to-pipe weld joint. The final step is to weld together and pump out the vacuum jacket, again using telescoping sections, orbital welders, and external leak checking.

A strand overlap distance of ~30cm is required to achieve 0.1 nΩ resistance in the splice. This corresponds to I^2R losses of 1W at 100kA. This length was estimated from joint resistance measurements of measurements of solder splices in SSC cables [25]. The actual joint resistance will be measured from the decay time of the current in the superconducting loop in the next prototype. If necessary, the splice overlap region can be increased to reduce the joint resistance, or additional superconductor can be added in the splice region.

Vacuum breaks are required at each end of the transmission line for the splicing scheme described above. This has the advantage that the vacuum integrity of long lengths of transmission line can be pre-tested in the factory, and the segments can be shipped into the tunnel already pumped down. An overall length of 1.5m and a heat leak of 1W are estimated for each of the two vacuum breaks.

12 MAGNET LENGTH

The optimum magnet length is still under consideration. The driving considerations are the cost and complexity of the magnet ends, the electrical power dissipation at resistive cryogenic joints, the layout of cabling and instrumentation on the magnet assembly, and the desire to minimize the work performed in the tunnel. All of these considerations argue for longer magnets. The arguments for a larger number of shorter magnets include the cost and complexities of handling long magnets and the cost of long assembly buildings.

The 50m prototype will provide several key inputs into this optimization. These include the electrical resistance which can be obtained at the transmission line splice, the heat leak that can be obtained at the vacuum breaks in the cryostat, and the ease or difficulty of dealing with long segments of iron. At present a magnet length of 250m (four half-cells) is contemplated.

13 EDDY CURRENT LOSSES

An area of concern which had not been addressed as of Snowmass was that of AC power dissipation due to eddy currents in the transmission line superconductor. This is of concern principally for the rapid cycling 3 TeV injector, which might also see duty as a continuously ramped fixed-target machine. A calculation has recently been performed [26] which indicates an average power dissipation of 50mW/meter for a very aggressive ramping scenario (10 second ramp time to 3 TeV, 40 second cycle time). This compares to the 100mW/meter anticipated for the heat leak into the transmission line cryostat, and does not appear to be a problem.

Field quality defects from conductor eddy currents and persistent current loops in the superconductor are not a problem for the superferric design. They are typically a major problem for conductor dominated superconducting magnets.

14 CRYOGENIC SYSTEM DESIGN

The cryogenic system has matured considerably since the work at Snowmass [27]. Work has focussed on the design of the 3 TeV injector system based on conventional NbTi conductor operating at 6-7°K. (The 50x50 TeV cryo system essentially replicates a very similar system).

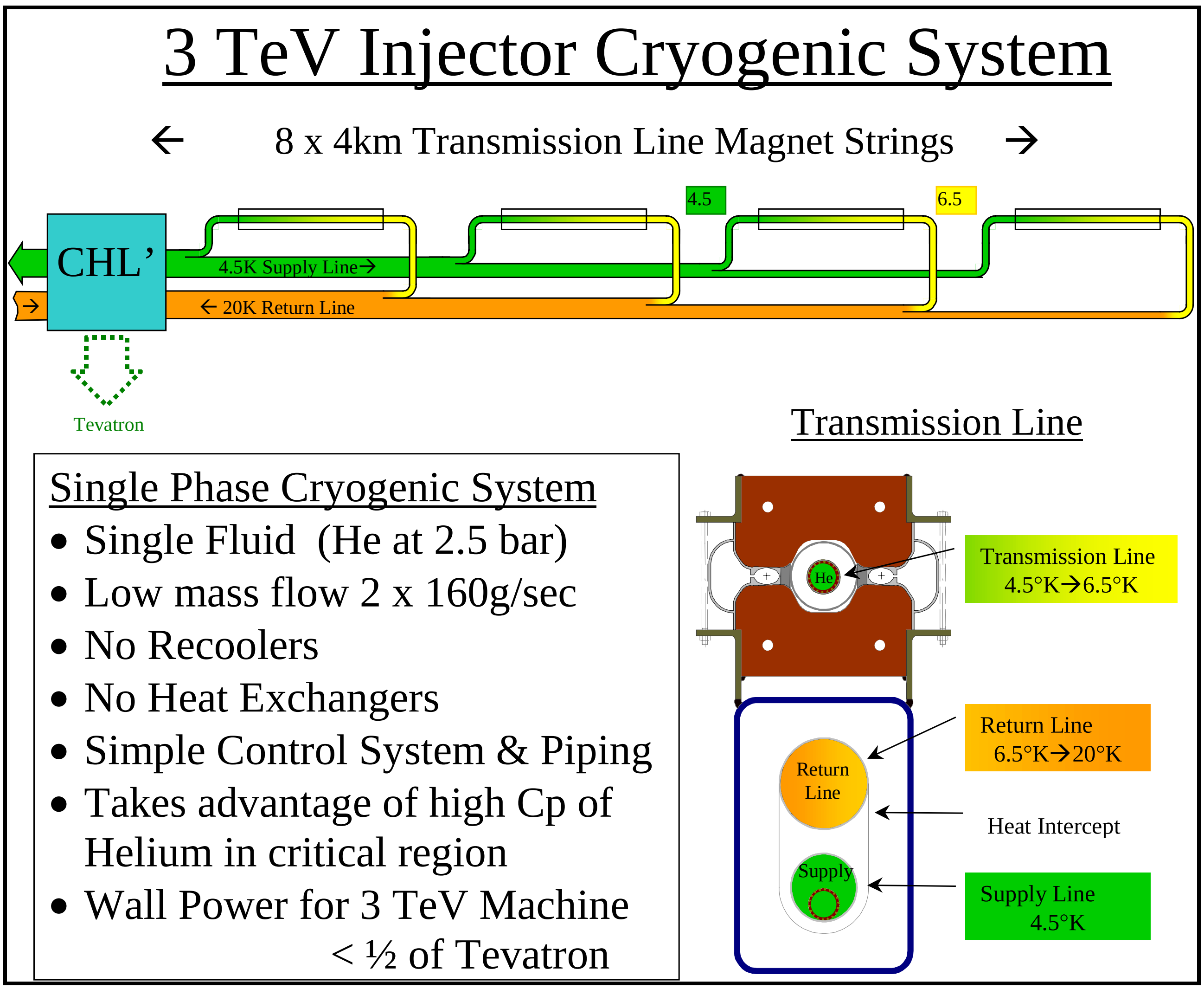

Fig. 15 – Cryogenic system for 3 TeV Injector. The 50x50 TeV cryosystem replicates this structure with 40km loops.

The cryogenic system is described more fully in the paper by McAshan [28]. It is a single-phase system with no recoolers or heat exchangers. A very simple control system is possible – of order 12 remotely operated valves for the 3 TeV cryogenic system. The system could be run from (a modified version of) the existing Fermilab Central Helium Liquifier (CHL) or a new cryo plant could be built. A very low power consumption system is possible if R&D goals for transmission line heat leak are achieved.

15 SUPERCONDUCTOR COSTS AND CHOICE OF OPERATING TEMPERATURE

The choice of operating temperature is a well-known tradeoff between superconductor costs and high-field performance (which favor a low operating temperature) and cryogenic complexity, capital and operating costs (which favor a high operating temperature). In many cases the operating field at the conductor has been pushed as hard as technologically feasible. Conductor costs have traditionally accounted for ~1/3 of total superconducting magnet costs. Thus historically this tradeoff has been resolved in favor of more costly and complex cryogenics systems and a lower operating temperature.

The situation for the VLHC is quite different. Firstly, the superconductor costs for 4.5K operation of the transmission line magnets represents only ~5% of the total cost of the magnets. There are several reasons for this. The iron-dominated design requires fewer ampere-turns per Tesla than a conductor-dominated (cosine-theta) magnet. The conductor itself operates at a low field (0.8T) so that a very high current density can be achieved. There has been almost an order-of-magnitude increase[29] in the current-carrying capability of NbTi conductors (at low field) since the time of the Tevatron. The transmission line magnet does not require the micron-sized filaments needed by cosΘ magnets, which lowers processing costs.

Secondly, the Carnot efficiency of refrigeration rises with operating temperature. This is directly reflected in electrical operating costs. The best predictor of cryo plant costs is the ideal wall power consumption of the system, so that these also scale with the Carnot efficiency.

Thirdly, a number of technological simplifications occur as the operating temperature is raised. At temperatures above 1.8K the complexities of a superfluid helium system are avoided. At temperatures above ~5K the recoolers and heat exchangers used in the Tevatron, SSC, etc. disappear. Thus there is considerable opportunity to trade increases in superconductor costs for decreases in cryogenic capital and operating costs by raising the temperature.

There are three components to the transmission line conductor costs: the transmission line conductor, the current return conductor, and the copper stabilizer.

The amount of transmission line conductor required scales inversely with the current density (Jc) in the conductor. At the temperature and operating field under consideration, Jc goes linearly to zero at ~8.8K. Thus for example raising the operating temperature from 4.4K to 6.6K will double the amount of transmission line conductor required. This raises conductor costs by about $400K/TeV.

The current return superconductor resides in the LHe supply line, which will operate at 4.5-5K in any scenario. Thus the return current (which represents half of the Ampere-meters in the magnet) does not scale significantly with operating temperature.

The copper stabilizer is far less expensive ($5/lb vs. $85/lb for the superconductor). The amount of copper stabilizer required is determined by quench protection and is essentially independent of temperature.

Our present understanding is that the single-phase cryo system operating at a peak temperature of 6-7K, using conventional NbTi conductor, is by a significant margin the lowest cost system for the transmission line magnet. This is discussed in more detail in Ref. 28.

16 THE RELEVANCE OF HIGH-TEMPERATURE SUPERCONDUCTORS AND Nb_3Sn

High-Tc Superconductors (HTS) have been considered and tentatively rejected for use in the VLHC. The main difficulty is that the projected conductor costs are far too high -- even if the R&D goals for superconductor production costs are met. The 5-year R&D targets for HTS are $10/kA-m (corresponding to $15M/TeV) which would more than double the magnet costs. Cryogenic system savings would not come close to covering this cost increase, even if the cryogenic system operated at 77K and was essentially free. In addition, there is a technical problem involving the DC power dissipation due to flux creep in HTS materials when operating near their rated J_C, which causes an unacceptably large cryogenic heat load. The result is that High Tc conductors must be operated at only about half of their rated quench current, thereby doubling the conductor costs. Another technical problem is that there is no known way of bypassing the quench current from the HTS material, aside from using the powder-in-tube conductors which contain an unaffordable amount of silver. In conclusion, it will require a major improvement in the technology, beyond what is hoped for in the short-term HTS R&D programs, before HTS conductor becomes economical for the transmission line magnet.

The situation for Nb_3Sn conductors is similar. A Nb_3Sn conductor could be operated at temperatures as high as 10-11°K, which results in substantial cryogenic savings. Because of this, there have already been extensive efforts commercialize the conductor for low field applications such as MRI. However the costs in large volume are roughly ten times the cost of NbTi. These represent mature production costs for volumes of conductor in excess of what is needed for the VLHC injector. Thus these efforts have largely failed to make

Nb_3Sn cost-effective for MRI despite its cryogenic advantages, and it will take an unanticipated breakthrough to make Nb_3Sn cost-competitive for the VLHC.

By far the most important development in superconductor for the transmission line magnet has already taken place, namely the order-of-magnitude increase in current density per dollar of conventional NbTi for low field applications. This was driven by the commercial interest in low-field (1-2T) applications such as MRI magnets. Continued development of NbTi conductors, particularly the commercialization of Artificial Pinning Center (APC) conductors[29], will no doubt continue to bring costs down. However conductor costs are already a sufficiently small part of the overall magnet costs (~$1-2M/TeV depending on operating temperature) that further conductor development is not required.

CRYOGENIC DISTRIBUTION LINES

A reference design has been adopted that is consistent with McAshan's parameters for the 3 TeV Injector cryo system[28]. The design of the distribution lines is more straightforward than that of the transmission line because of the absence of large conductor forces and the larger radial space available for superinsulation and radiation shields. A cross section is shown in Fig. 16. The supply and return flows (both single phase supercritical He at 2-3 bar) are carried in 3" and 4" OD stainless tubing.

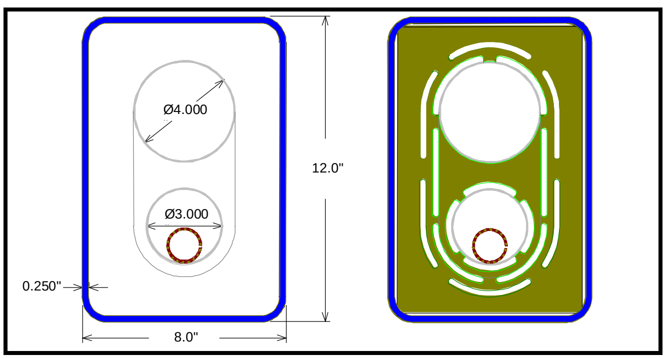

Fig. 16 – The cryogenic supply and return lines inside the structural support beam/vacuum jacket. The 3" LHe supply line contains the current return. A thermal shield connected the 4" return line protects the supply line from radiative heat loads. A 3cm thick blanket of superinsulation (not shown) is wrapped around the cold mass. The G-10 support "spider" built for the 2m prototype is shown at right. Other support geometries (such as slings or support posts) are also under consideration.

Fig. 17 – Photograph of the cryogenic supply and return lines of the 2m prototype. Dimpled aluminized Mylar is wrapped around the 2-pipe package as well as the smaller 3" supply line.

The cryo distribution lines are a conventional all-welded system with bellows and flow liners (Fig. 18) every 40ft to handle thermal contraction. The design and manufacture of these cryogenic lines are similar to others used at Fermilab for years[30].

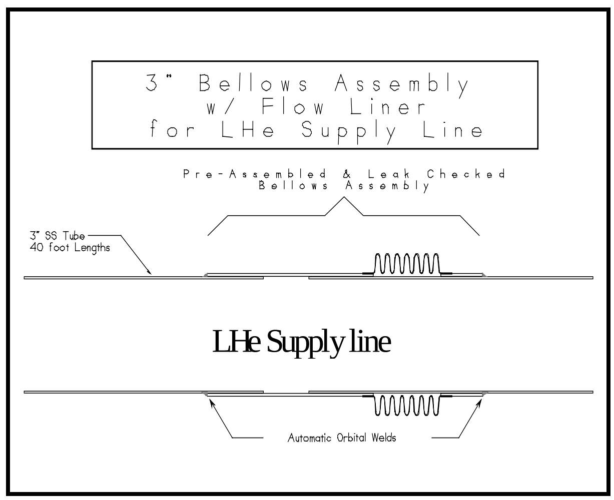

Fig. 18 - Bellows assembly for cryogenic supply lines. The bellows allows for thermal contraction of each 40ft length of pipe. The tubes are supported in a semi-rigid coaxial telescoping geometry. A relatively smooth inner bore maintains low hydraulic impedance. A useful feature of this design is that does not require exactly cut lengths of 40ft tubing.

The supply line is shielded by an aluminum heat intercept which is in thermal contact with the return line. Thus ambient heat is intercepted into the return line instead of the supply line, and the delivery temperature of cryogens to the magnet string is not strongly affected by variations in the effectiveness of the superinsulation on the cryogenic lines. This also ensures a maximum temperature below 5K in the current return conductor carried in the supply line.

A design variation under consideration is to cool the shield with a separate gaseous-He cooling line operating in the 30-80K range. This would reduce operating costs and insulation requirements but increase the number of pipes to three and increase overall system complexity.

Alternate materials are being considered for the cryogenic transfer lines. These include corrugated stainless or aluminum piping, and Invar. These materials have the potential for eliminating bellows from the cryogenic lines. At present it appears that the conventional (welded stainless pipe + bellows) approach is the lowest cost.

In the present design the cryo line vacuum jacket also functions as the support beam for the magnet assembly. An alternative is to place the cryo distribution lines in a separate mechanical pipe. This has the benefit of de-coupling the installation and maintenance of the cryo line from the rest of the magnet, and perhaps allowing somewhat longer lengths of cryogenic line to be installed in single pieces. The fluid flows interconnect only every ~4km (see Fig. 15). The present approach has the advantage of holding the return conductors in a reproducible location, and making all conductor-to-conductor forces self-contained inside the magnet assembly.

Also under consideration is replacing the rectangular structural tube with a round pipe. Round pipe (as opposed to rectangular structural tube) comes with an implied warrantee of not leaking. It can be obtained in the certified clean, oil-free condition that is needed for a vacuum jacket. It is more straightforward for automatic equipment to weld and inspect. The twist tolerance for rectangular tube is not an issue with round piping. The arguments against a round vacuum jacket are that it needs more wall thickness than a rectangular tube to achieve the same structural stiffness, and that the overall assembly looks sort of peculiar.

17 HEAT LEAK TESTS

One of the most cost-effective R&D activities on the transmission line magnet is the demonstration of low heat leaks in a manufacturable structure. Using generic costs for superinsulation performance (heat leak ~1 W/m^2) and cryo plant costs (~$1k per watt at 4.5K Carnot equivalent), we find that cryogenic plant costs are roughly half of magnet costs. If a lower heat leak can be demonstrated this goes almost directly into reduced cryo plant operating and equipment costs.

We have performed preliminary tests of a promising new superinsulation material[31] using large-crystal aluminum to achieve ultra low infrared emissivity. These tests used the superinsulation test stand developed at Fermilab for SSC tests[32].

We are designing a dedicated superinsulation test fixture to measure and optimize the performance of insulation and support structures in a transfer line geometry. This system will rely on measuring the rate of LHe boil-off to determine the heat flux leaking into a sample of transmission line. See Fig. 19.

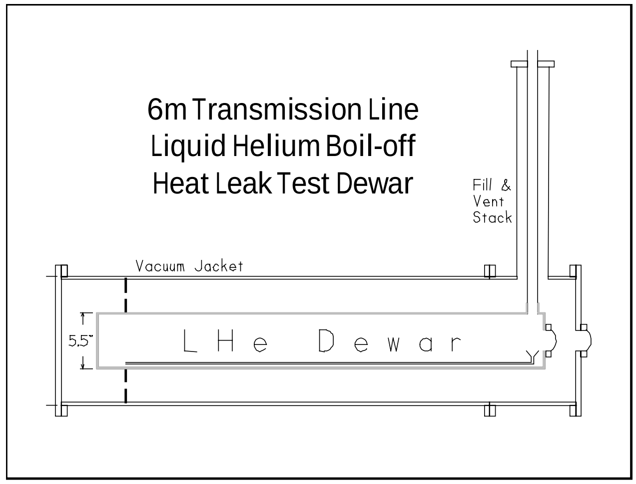

Fig. 19 – Test Dewar to measure heat leak of transmission line using LHe boil-off rate.

The boil-off approach has been chosen because it can reasonably be extended to long prototype magnet assemblies. The initial tests will concentrate on the 4" diameter lines for the cryo distribution pipes which dominate the heat leak. Our goal is to reproduce the best published results[33] of ~0.3 W/m^2 with an insulation and support design compatible with mass production of transmission line.

18 POWER SUPPLY AND QUENCH PROTECTION

The power supply and quench protection system for the 3 TeV machine (Fig. 20) is almost identical to one half-sector of the 50 TeV machine described by Koepke et. al. [34].

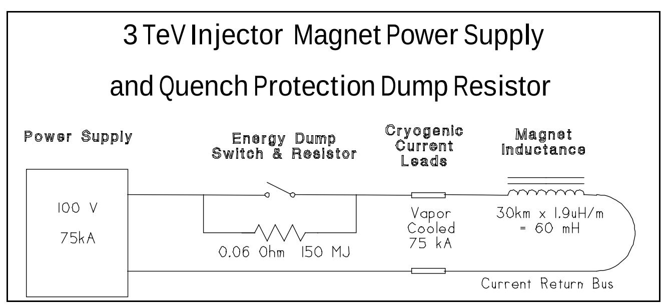

Fig. 20 – Power Supply and Dump Circuit for 3 TeV Injector.

The VLHC power supply is greatly simplified by the low inductance of the 1-turn magnet. This enables the entire magnet string to be treated as a two-terminal device (a single lumped inductance). In contrast, the Tevatron is something like a 12-Terminal device, with non-negligible distributed capacitance.

The power supply and dump circuit are located in a service building upstairs. They are connected to the magnets by a length of superconducting transmission line carried inside the cryogenic transfer lines. There are no remote power supply buildings. Among other benefits, this reduces the number of possible entry points for power supply noise which could affect beam emittance growth.

The power supply voltage depends on the ramp time chosen, which depends on the physics mission of the machine. The 100V supply in Fig. 20 will provide a 40-second ramp time for the 3 TeV machine. For this ramp rate 7.5MVA are required or about 1/12 of the Main Injector. Steady-state power dissipation at full current comes primarily from voltage drops in the power supply output filter, copper bus work, dump switch, and current leads and is estimated to be 1.5 MW.

A dump time constant of 1 second has been chosen. This corresponds to a maximum voltage of ±2kV to ground during a full-current dump. Longer dump times reduce this voltage but require more copper stabilizer in the transmission line drive conductor.

The dump switch is based on the Tevatron dump switch. As in the Tevatron, the switch will consist of two switches in series: an electronic switch which opens immediately, and a electromechanical switch which opens a few milliseconds later and serves as a fail-safe backup for the electronic switch.

The design of the electronic switch for the 3 TeV dump is simplified by the use of Gate-Turn-Off (GTO) SCR's which were not available at the time of the Tevatron. The design will become even easier when MOS-Controlled Thyristors (MCT's) become available with appropriate voltage and power ratings. These eliminate the obnoxiously large drive currents required to turn off GTO's.

The dump resistor itself is an appropriately scaled length of stainless steel. A thermal mass of 1 Ton is required for a 375°C rise in temperature from a full current quench.

The 75kA cryogenic current leads are larger than those used for HEP magnets but are comparable to leads developed for Superconducting Magnet Energy Storage (SMES) applications [35]. The development of High-Tc leads will be useful but not essential reduction in the operating costs since there are only one set of power supply leads in the machine.

19 ELECTRICAL TRANSMISSION LINE MODES

Treating the entire string of transmission line magnets as a single lumped inductance requires that the electrical propagation delay through the magnet chain be small compared to the start and stop times of the ramp. To evaluate this, a SPICE simulation[36] of the transmission line and current return system was performed. Mutual and self-inductances and capacitances were estimated from the transmission line geometry, and a subcircuit was developed representing a unit length of transmission line. Only a single dissipative source was included, namely the eddy-current losses in the stainless vacuum jacket of the transmission line.

The result of the SPICE simulations was that the transmission line magnet string for the 3 TeV machine can be treated as a single lumped inductance up to frequencies of ~500Hz. At this frequency the first transmission line resonance appeared, with a Q of ~10. By comparison, a similar simulation for one sector of the Tevatron magnets correctly predicts the first transmission line resonance at ~70Hz. The conclusion is that transmission line effects should be negligible for the frequency components present in a 10 second (or longer) ramp times under discussion for the 3 TeV machine.

20 VACUUM SYSTEM

The vacuum system of the transmission line magnet is an extruded-aluminum system similar to many electron machines. Primary pumping is provided by Non-Evaporable Getter (NEG) strips located in a high-conductance antechamber (see figs. 1,2). Lumped sputter-ion pumps are required every ~100m to pump methane and noble gasses (which are not pumped by the NEG strip). The design is reviewed in the Snowmass proceedings [37].

A custom aluminum extrusion and a vacuum test system are being built by our Japanese collaborators at KEK this fall. Their industrial partner is Ishikawajima-Harima Heavy Industries (IHI) who were responsible for fabricating the aluminum vacuum system for the SPring-8 light source. IHI has performed a finite-element analysis and several design optimizations are being made. Support for a continuation and expansion of this collaboration has been applied for as part of the US-Japan accord.

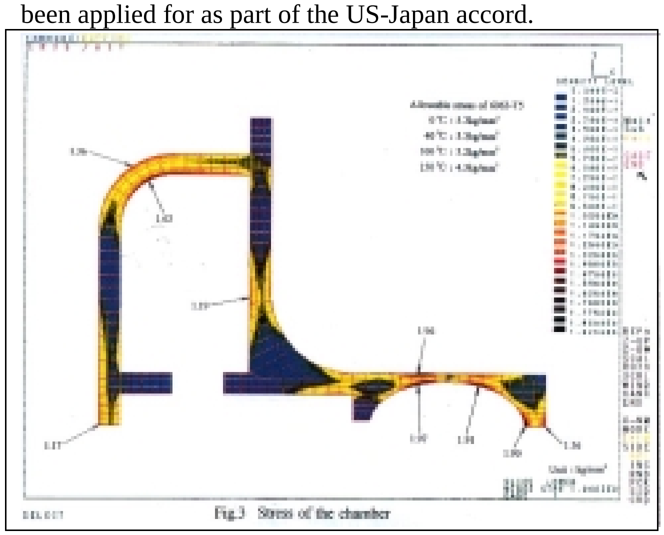

Fig. 21 Finite-element stress map of the VLHC beam pipe extrusion performed by IHI. Yielding of the Aluminum is an issue because of the elevated bakeout temperature, the use of high-purity aluminum, and the desire for as thin an extrusion wall as possible in the region immediately above the beam.

An attractive scheme for installing and supporting the long lengths of NEG strip in the vacuum chamber has been developed. The NEG strip will be double insulated and supported by a silica-coated aluminum U-channel. This technique should allow the NEG strip to be pulled down the 65m free length of extruded beam pipe between BPM/Pump assemblies. The outgassing rate of the silica coating is low and the insulation and mechanical properties are excellent.

Two extremely useful developments in the NEG strips have occurred of the last couple of years. The first development is that the SAES patent on NEG strip has expired, resulting in increased competition and a dramatic drop in price[38]. The second development is that lower activation temperature getters have been demonstrated[39]. This simplifies the getter strip regeneration procedures.

A bellows-free vacuum system [40] is planned and must survive modest bakeout temperatures of ~85°C. Finite element analyses [41] indicate that the longitudinal stress in the aluminum stays below allowable limits provided the compressive load is appropriately transferred to the magnet and support beam.

21 INSTRUMENTATION

The low-field VLHC contains two classes of instrumentation: the "once per turn" instrumentation, and the equipment that is distributed repetitively around the circumference. The "once per turn" instrumentation for the 3 TeV machine is discussed by A. Hahn in Ref. 42. Essentially everything can be copied (or recycled) from the Tevatron. This equipment will be housed in the on-site straight section and its installation and maintenance will be similar to existing operations.

The instrumentation distributed around the ring is discussed and enumerated in [43]. This equipment dominates the electronics costs. An important feature of the VLHC design concept is that this instrumentation, which occurs in "lumps" every half- cell (~65m for the 3 TeV machine, longer for the 50x50 TeV machine), is to be integrated into the long length magnets. Instrumentation is pre-assembled, cabled, and tested before the magnet is transported into the tunnel. The only tunnel installation jobs are the electrical connections at the ends of the magnets for power distribution and the fiber optic network links. This minimizes the requirements for and costs of tunnel infrastructure around the circumference.

An aluminum-shelled beam position monitor (Fig. 23) with an aperture appropriate to the transmission line magnet has been built by our Japanese collaborators. It is a split-tube device with the inner electrodes plated onto a ceramic shell. This is being tested at FNAL to determine if the electrical parameters, beam impedance, and linearity (response map) are suitable.

The device fits inside a slightly enlarged magnet gap (with about 2/3 the nominal bend field) in modified section of steel 15cm long. Thus the loss in dipole filling factor from the BPM's will be only ~5cm. The sputter-ion vacuum pumps, NEG activation feed-throughs, and pump out ports will be housed in a "unit chamber" at each BPM location. These vacuum connections will not interrupt the bend field.

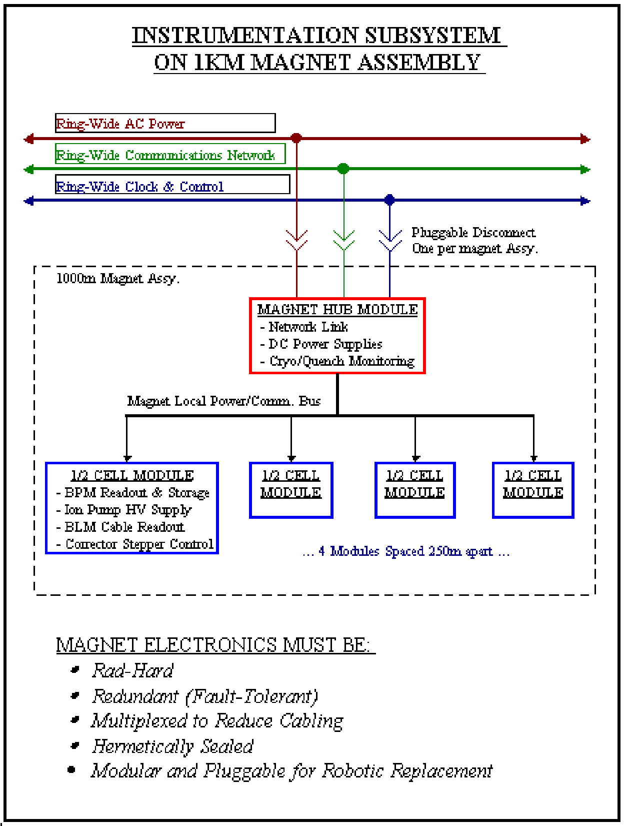

Figure 22 – Schematic instrumentation layout on the transmission line magnet. Instrumentation is lumped at each half-cell location (shown here for 250m half-cell spacing for the 100 TeV machine). The instrmentation is multiplexed onto a small number of ring-wide digital links, which can be in either a "star" or "ring" topology. The instrumentation "lumps" are discussed in Ref. 43.

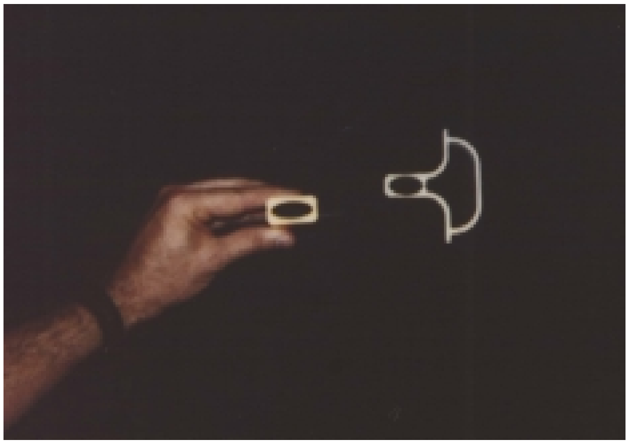

Fig. 23 – Photograph of the aluminum shelled split-tube BPM and an aluminum beam pipe test section.

Beam-loss monitors are needed which span the length of the transmission line magnet. Tevatron-style ionization chambers work well, are radiation resistant, hermetically sealed and require no maintenance.

However a large number of these would be required to span the 75m between half-cells without the possibility of blind spots. Cable-style loss monitors provide continuous coverage but require gas flow because of the plastic shell. The best of both worlds should be attainable with a gas-filled rigid coax cable with a solid aluminum shell as the outer conductor. This rigid coax will be installed and transported as part of the long magnet assembly. We will perform tests to determine if such a rigid-coax BLM can be adequately sealed and thereby maintain an indefinite service life.

22 THE NEXT PROTOTYPE

Design work and parts ordering has begun on the next ~50m long prototype magnet[44]. The goal is to realistically test a complete magnet assembly, i.e. one which simultaneously meets all design constraints involving conductor performance, thermal contraction, magnetic forces, alignment, conductor splicing, and vacuum breaks at the magnet ends. At present we are not adding to this list the crenellated iron shape which will provide the ultimate field quality; this is being pursued in parallel on the iron test stand. When the iron shape is fully developed then the iron structure on the prototype can be easily replaced.

Three methods of driving the prototype 75kA transmission line were considered. The system components are being designed to 100kA capability to provide adequate design margin and the ability to drive the iron deep into saturation.

The first method considered was to use a pair of 100kA current leads and a 100kA power supply. The system would look very much like the final power supply configuration in Fig. 20. This would however cost of order $1M and many man-months of design work. It would require a direct connection to the Fermilab's Central Helium Liquefier (which will not be running in the next 12 months) and would require a substantial support crew. It has the advantages that the power supply & leads would be usable for arbitrarily long string tests and (depending on the voltage and required ramp rate) could be usable as the ramping supply and current leads for the 3 TeV injector. These supplies would allow us to "beat up" on the magnet by ramping continuously, etc.

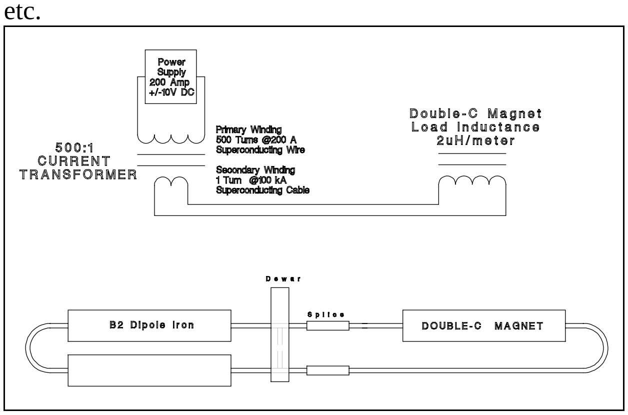

Figure 24 – An alternative considered for driving the next transmission line prototype. The current transformer approach of the first prototype would be scaled up using B2 magnets leftover from the Main Ring as the transformer cores. The primary winding would be 500 turns of superconducting strand wire in a shared cryostat with the transmission line.

A second method considered was to scale up the existing current transformer setup, but make a primary winding using superconducting strand at modest current (e.g. 500 turns at 200 Amps). Existing magnet cores (B1's or B2's from the Fermilab Main Ring) would be used as the transformer cores. The advantage of this approach is that the system can remain Dewar-based since no high current (and high Helium consumption) leads are needed. A further advantage is that a small rack-mounted 200 Amp power supply is sufficient to charge the magnet. A disadvantage of the system is that a rapid ramp rate cannot be achieved since the voltage on the primary becomes prohibitive. Quench protection of the multi-turn primary winding is also an issue.

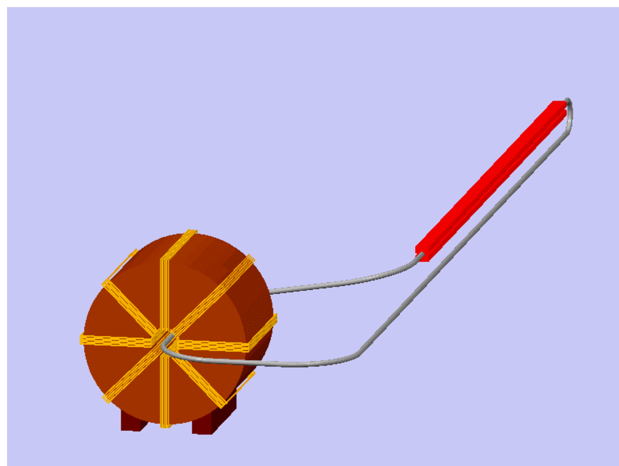

Fig. 25 – Use of a surplus fixed-target analysis toroid magnet as the drive transformer to power the next (50m) prototype magnet. This is a direct scale-up of the technique used in the first prototype. The system will be set up in the MP8 tunnel upstream of the MP9 Permanent Magnet Factory.

The third (favored) method considered was to scale up the existing current transformer setup, with more Ampere-turns on a water-cooled-copper primary and more iron in the transformer core. A breakthrough was made with Jim Volk's suggestion that an existing analysis toroid from a fixed-target experiment could serve as both the transformer core and primary winding for the flux transformer. See Fig. 25. The superconducting transmission line would be looped through the toroid, and the 100kA current would be excited when the toroid was energized. The total magnetic flux (volt-seconds in the transformer core) of an existing (MW9) toroid would be sufficient to power a 50m test magnet. This system will be limited to a ramping time of 10-20 seconds due to the solid iron core of the toroidal transformer.

The cryogenic system for the 50m prototype will benefit from several lessons learned from the first prototype. These include the need for a more mechanically robust conductor, the desirability of designing vessels in diameters below 6" so that piping codes (instead of pressure-vessel codes) apply, and the desirability of forced flow and controlled venting of warm gas during cool-down.

The convective "bubble-pump" approach used in the short transmission line prototype will not work for the 50m magnet. The current plans are to attempt the simplest possible LHe transfer scheme, which is to force-flow single phase liquid from a Dewar into one end of the loop and to discharge 90%gas/10% liquid out the other end of the loop. The transfer rate will be regulated to control the level of liquid in a vertical phase separator column at the end of the loop. There is some possibility that this simple system may become vapor-locked. In this case it will be necessary to install an inline pump to recover and recycle the liquid from the phase separation column, and pump it back into the head of the transmission line. Such a pump will be necessary in any case when we convert the transmission line test to single-phase (supercritical fluid) operation to study the behavior of the conductor at elevated temperatures.

REFERENCES

[1] 'The Pipetron, a Low-Field Approach to a Very Large Hadron Collider' [The Pink Book], selected reports submitted to the Proceedings of the DPF/DPB Summer Study on New Directions in High-Energy Physics (Snowmass '96), compiled by Ernie Malamud (malamud@fnal.gov) Jan 1997. Current project information can be found at http:://www-AP.fnal.gov/PIPE and ../VLHC

[2] G. W. Foster, P. O. Mazur, T. Peterson, C.D. Sylvester, P. Schlabach, "Design and Operation of an Experimental "Double-C" Transmission Line Magnet", presented at PAC '97.

[3] "Magnetic Calculations for the Transmission Line Magnet and Current Transformer Test Setup", G.W. Foster, FNAL Tech. Div. Note #TD-97-014.

[4] G. W. Foster, 'Magnetic Calculations for the Pipetron Transmission Line Magnet', in Ref. 1.

[5] The crenelation technique was described by R.R. Wilson in the 1982 Snowmass proceedings. He describes it as "an old idea". Stan Snowdon evaluated it numerically and wrote a 1983 Fermilab TM on the subject. As far as I can tell it has never been tried experimentally.

[6] A. Makarov, Design notes for the water-cooled copper Double-C magnet test stand. FNAL Tech. Div. Drawing #.

[7] "Magnetic Forces on the Transmission Line Drive Conductor", G.W. Foster (in preparation). Mechanical support and rigidity issues are addressed in M. McAshan's writeup on the 3 TeV Cryosystem.

[8] "A 2-in-1 Lambertson Magnet for VLHC beam Transfers", G.W. Foster Aug 1997.

[9] S. Mishra, "Lattice Design for the 3 TeV Low Field Injector", contribution to the FNAL 1997 VLHC summer study.

[10] G. W. Foster, "Aperture Requirements for the Low Field VLHC and Injector", contribution to the FNAL 1997 VLHC summer study (in preparation).

[11] J. Marriner, "A Damper to Suppress Low Frequency Transverse Instabilities in the VLHC", contribution to the FNAL 1997 VLHC summer study.

[12] TMCI note (in preparation).

[13] Examples of this are the CESR magnets and the (calculated) performance of the FNAL Main Injector and Recycler magnets. The acceptance of these machines is limited by the vertical physical aperture, not the field quality of the iron magnets.

[14] V. Shiltsev, "Pipetron Beam Dynamics with Noise", contribution to the FNAL 1997 VLHC summer study

[15] G. P. Jackson private communication.

[16] "Local Alignment Tolerances in the Transmission Line Magnet", G.W. Foster, contribution to the FNAL 1997 VLHC summer study.

[17] T. Murphy, "Alignment of the 3 TeV VLHC Injector", contribution to the FNAL 1997 VLHC summer study.

[18] "Slow Extraction from the 3 TeV Injector to the VLHC", J.Marriner, contribution to the FNAL 1997 VLHC summer study.

[19] S. Mishra, "Lattice Design for the 50x50 TeV Low Field VLHC.

[20] Zhijing Tang, "ANSYS Calculation of the Eddy Current Field Defects in the VLHC Transmission Line Conductor", presentation to the VLHC low field magnet design group, 1996.

[21] "Local Alignment Tolerances in Transmission Line Magnet Assembly", G. W. Foster, contribution to the FNAL 1997 VLHC summer study.

[22] Invar is a trade name for 36% Nickel steel, available from Carpenter Technologies (formerly Carpenter Steel) and a number of other vendors.

[23] Tom Moreland (a FNAL Beams Division Engineering co-op student) is writing his term report on thermal contraction issues in the drive conductor.

[24] The external leak-checking technique developed by P.O. Mazur of Fermilab involves a disposable rubber seal which makes the clamshell leak-checking possible.

[25] M. Kuchnir, measurements of SC splice resistances in IEEE magnetics last year.

[26] "Eddy Current Power Loss in the VLHC Transmission Line Conductor", Iouri Terechkine Sept. 1997.

[27] M. McAshan, P.O. Mazur, "Cryogenic Systems for the Low Field RLHC Study Cases", in Ref. 1.

[28] M. McAshan, "Cryogenic Systems for the 3 TeV Injector Study".

[29] D. Larbelestier and P. J. Lee, "New Developments in Niobium Titanium Superconductors", proceedings of the 1995 Particle Accelerator Conference (Dallas).

[30] P-West Transfer Lines at FNAL use this bellows arrangement.

[31] Dr. H. Ishimaru of KEK provided us with samples of large grain size aluminized Kapton for these tests.

[32] "Design and Calibration of a Test Facility for MLI Performance Measurements Below 80K", W. Boroski et. al., FNAL, Proc. CEC/ICMC Conf. Huntsville AL. June 1991.

[33] T. Ohmori et. al., "Multilayer Insulation with Aluminized Dimpled Polyester Film" (Solenoid Cryostat for the Venus experiment at KEK) in Proc. 11th Intl. Cryogenic Engr. Conf., Berlin, April 1986. Somewhat better results are reported in R.J. Stochl, et. al. "Variable Density MLI Test Results" , Adv. Cryo. Engr. 41a, Plenum 1996.

[34] K. Koepke, A Zlobin, G.W. Foster, "Power Circuit and Quench Protection for the Pipetron Transmission Line Magnet", in Ref. 1.

[35] There are a set of 65-kA current leads in a test setup at the University of Wisconsin, for example.

[36] Dan Wolff of FNAL performed the SPICE simulations under the direction of Karl Koepke. I have copies of his notes and intend to scan them in and put them on our Web server.

[37] William C. Turner, "Beam Tube Vacuum in Low Field and High Field Very Large Hadron Colliders", in Ref. 1, also LBNL-39482, UC-414.

[38] Currrent pricing for NEG strip in large quantity is between $10-$20/m. W. Chou tells us that the Advanced Photon Source at ANL previously paid $120/m.

[39] Benvenuti et. al, recent CERN preprint.

[40] H. Ishimaru, "Conceptual Design for a Very Low Cost Aluminum Alloy Vacuum Chamber in a High Energy Low-Field Collider", in Ref. 1.

[41] H. Ishimaru, presentation to the VLHC low field magnet working group.

[42] A. Hahn, "Single point beam insrumentation for the 3 TeV Injector", contribution to the FNAL 1997 VLHC summer study.

[43] B. Goodwin, P. Lucas, E. McRory, M. Shea, "Controls and Instrumentation for the 3 TeV Booster to the VLHC", contribution to the FNAL 1997 VLHC summer study.

[44] "Design Parameters for the Next Transmission Line Magnet Prototype" , G. W. Foster (in preparation).